Optimal Solar Sail Transfer to Linear Trajectories

Alessandro A. Quarta, Giovanni Mengali, *

Dipartimento di Ingegneria Aerospaziale, University of Pisa, I-56122 Pisa, Italy

Abstract

The aim of this paper is to characterize a mission toward a heliocentric linear trajectory (that is, a rectilinear orbit) and to investigate the performance of a solar-sail-based spacecraft to accomplish the transfer phase. A similar problem has been recently discussed under simplified assumptions, but new results are now provided with a thorough analysis that uses a three dimensional transfer orbit and a piecewise constant steering law. The paper investigates a complex mission scenario, where the solar sail returns back to Earth after a scientific probe is released along a target linear trajectory.

The employment of a propellantless propulsion system for such a mission is encouraged by the high velocity variations, usually greater than 15 km/s, required by a conventional bi-impulsive transfer. The paper shows that a rectilinear orbit, for a candidate scientific mission dedicated to the study of the circumsolar space, can be reached with a solar sail of high performance. In particular, the insertion of an ideal, flat solar sail into a rectilinear orbit with an aphelion radius of 5.2 AU requires a characteristic acceleration of about $3.52\,\mathrm{mm/s^2}$ and a flight time of 2.85 years. This is a rather demanding requirement, which is well beyond the current technology capabilities. However, it is significantly smaller than the value required by other exotic missions, such as those regarding the attainment of heliostationary orbits or those involving the orbital angular momentum reversal.

Key words: Rectilinear orbits, H-reversal, Solar sail

* Corresponding author.
Email addresses: a.quarta@ing.unipi.it (Alessandro A. Quarta,), g.mengali@ing.unipi.it (Giovanni Mengali,).

1 Nomenclature

A = sail area [m^2]

a_c = spacecraft characteristic acceleration [$\mathrm{mm/s}^2$]

$\widetilde{a}_c$ = characteristic acceleration of the solar sail alone [$\mathrm{mm/s}^2$]

i = orbit inclination [deg]

m = mass [kg]

n = number of revolutions

$P_\oplus$ = solar radiation pressure at 1 AU [$\mathrm{N/km}^2$]

r = radial distance [AU]

t = time [years]

u = radial velocity component [km/s]

v = transverse velocity component [km/s]

α = sail cone angle [deg]

γ = heliocentric latitude [deg]

ΔV = velocity variation [km/s]

η_p = probe mass fraction

θ = polar angle [deg]

λ = heliocentric longitude [deg]

$\mu_\odot$ = Sun's gravitational parameter [$\mathrm{km}^3/\mathrm{s}^2$]

Subscripts

a = aphelion

p = probe

s = solar sail

$0 \quad = \quad$ initial

$1 \quad = \quad$ probe's release

$2 \quad = \quad$ probe's destruction

$3 \quad = \quad$ Earth's rendezvous

$\oplus \quad = \quad$ Earth

2 Introduction

In a recent paper [1], Quarta and Mengali have characterized a mission toward a heliocentric Elliptic Rectilinear Orbit (ERO) belonging to the ecliptic plane, and have investigated the capabilities of a solar-sail-based spacecraft to accomplish the transfer phase within a two-dimensional framework. The use of a linear trajectory to perform a close approach to the Sun, and obtain an in-situ observation of charged particles, magnetic fields, and gravitational harmonics, was proposed in 1976 by Colombo et al. [2]. The main advantage of a linear orbit is that its peculiar shape simplifies the design of both the thermal and attitude control systems of the scientific probe [2].

The employment of a propellantless propulsion system for such a mission is encouraged by the high velocity variations required by a conventional (high-thrust) multiple-impulse transfer. To obtain a rough estimate of the required ΔV, consider a Hohmann-like (bi-impulsive) two-dimensional transfer from a circular heliocentric orbit of radius $r_\oplus \triangleq 1\,\mathrm{AU}$, like that shown in Fig. 1(a), toward an ERO with aphelion distance $r_a > r_\oplus$. This transfer requires a total ΔV of a few dozen kilometers per seconds, see Fig. 1(b).

According to Ref. [1], a rectilinear orbit for a candidate scientific mission dedicated to the study of the circumsolar space can be reached with a high performance solar sail. For example,

the insertion of an ideal, flat solar sail into a rectilinear orbit with an aphelion distance of $r_a = 5.2\,\mathrm{AU}$ (equal to the mean distance between Earth and Jupiter) requires a characteristic acceleration a_c of about $3.52\,\mathrm{mm/s^2}$ [1]. Note that a_c is, by definition, the maximum propulsive acceleration calculated at a Sun-sail distance equal to $r_\oplus$. Because the value of $3.52\,\mathrm{mm/s^2}$ is obtained assuming a perfectly reflecting sail, the question arises of estimating the mission performance degradation when the thermo-optical characteristics of the sail film are take into account. This problem can addressed using an optical force model [3,4]. The simulations show that the previous value of a_c grows up to $3.68\,\mathrm{mm/s^2}$, with a 4.5% increase only with respect to the ideal sail based model. Therefore it can be concluded that the optical characteristics of the sail film have a negligible effect on the transfer performance for this kind of mission.

Figure 2 shows that the minimum value of the characteristic acceleration required to reach an ERO with the aphelion radius ranging in the interval $r_a \in (1,\ 10]\,\mathrm{AU}$ is greater than $2.5\,\mathrm{mm/s^2}$. This is a rather demanding requirement, which is well beyond the current technology capabilities. However, such a value is comparable or, in some cases, even significantly smaller than the value required to accomplish other exotic missions, such as those regarding the attainment of heliostationary orbits [5,6] or those involving an orbital angular momentum reversal [7,8]. In addition, Fig. 2 also shows that the flight time t_1 is on the order of a few years, a value comparable with those obtained in Hohmann-like bi-impulsive transfers. Note that Fig. 2 involves an ERO insertion at aphelion, a situation in which the solar sail reaches the target linear orbit with zero radial velocity.

The aim of this paper is to analyze a realistic mission scenario in which the insertion of a scientific probe into an ERO is completed by the presence of an extended mission phase. The latter involves, as an example, a return mission toward the Earth whose aim is to investigate the effects on the sail film of a prolonged exposition to the interplanetary environment. Another possible extended mission application, currently under development, is represented by an escape trajectory from the Solar System using the H-reversal concept introduced by Vulpetti [7,8].

The paper is organized as follows. First, a typical scenario for a two-dimensional mission to a heliocentric linear trajectories is illustrated [1], and the effect of a simplified, piecewise-constant, control law is studied. Then, a mission concept involving a solar sail return to Earth is introduced, and a description is given of the phases into which the whole spacecraft trajectory can be divided. For each mission segment the different parameters that influence the trajectory shape are discussed (such as the propulsive acceleration, the flight time and the aphelion distance), and a tradeoff analysis between the various sub-phases is performed in a two-dimensional, optimal, framework. As a result, an estimate of the performance required by a flat solar sail to accomplish the whole mission is presented in graphical format. Finally, a fully three-dimensional scenario is analyzed and the effect of the ERO inclination on the mission performance is calculated.

3 Mission toward a rectilinear orbit

Consider a space vehicle whose primary propulsion system is a flat solar sail. At the initial time $t_0 \triangleq 0$ the spacecraft follows a circular heliocentric orbit of radius $r_\oplus$. When the eccentricity of the Earth's heliocentric orbit is neglected, the previous situation is representative of a space vehicle at the end of an Earth-escape phase with zero hyperbolic excess velocity with respect to the planet. According to Ref. [1], the reference problem consists of finding the minimum characteristic acceleration a_c required to reach, within a given time t_1, the aphelion of an ERO coplanar to the starting orbit. The coplanarity assumption is useful to obtain an estimate of the minimum solar sail performance necessary to attain the rectilinear orbit. However, the mission analysis will be further refined in the second part of the paper when a fully three-dimensional scenario will be discussed. The minimum value of a_c is found with an indirect approach, following the methodology described in Ref. [9]. Note that the aphelion distance r_a is an output of the optimization process.

The numerical values $a_c = a_c(t_1)$ and $r_a = r_a(t_1)$, which relate the minimum characteristic acceleration and the aphelion distance with the flight time, are obtained by repeatedly solving the above problem for different values of the flight time t_1. The corresponding results can be displayed in graphical form as shown in Fig. 2. A typical transfer trajectory is illustrated in Fig. 3, which shows the optimal trajectory necessary to reach an ERO with an aphelion distance $r_a = 5.2\,\mathrm{AU}$. In this case the flight time is about 2.85 years, see Fig. 2. Figure 4 illustrates the time histories of r, u, and v, which, respectively, represent the Sun-sail distance and the radial and transverse components of the spacecraft absolute velocity. Note that an insertion into an ERO at aphelion requires that $u(t_1) = v(t_1) = 0$.

4 Solar sail steering law

The previous trajectory can be tracked by a solar sail with a characteristic acceleration $a_c = a_c(r_a)$ only if the sail attitude is continuously varied in such a way to suitably orient its propulsive thrust direction. In fact, both the thrust direction and its modulus depend on the sail cone angle $\alpha \in [-90,\, 90]\,\mathrm{deg}$, that is, the angle between the incoming rays direction and the normal to the sail nominal plane, see Fig. 5. A negative value of α means a propulsive thrust with opposite direction with respect to the spacecraft transverse velocity. Figure 5 shows the cone angle time history for the mission drawn in Fig. 3. Note that the cone angle takes a value that remains nearly constant, roughly $\alpha \simeq -30\,\mathrm{deg}$, during most of the sailing mode (about 70% of the propelled phase). Such a value of cone angle is close to the optimal value $\alpha = -\arctan(1/\sqrt{2}) \simeq -35.26\,\mathrm{deg}$ that minimizes the transverse component of the propulsive thrust for an ideal sail force model [4].

The time history of the cone angle suggests a possible simplification of the solar sail steering law. In fact, recalling that α attains a nearly constant value during most of the propelled phase, it is reasonable to resort to a piecewise-constant steering law [10] whose aim is to substantially

reduce the complex task of continuously reorienting the sail along the spacecraft trajectory. The mathematical model necessary to study the mission performance with a piecewise-constant steering laws is similar to that discussed in Ref. [10], and is based on the discretization of the admissible variation range of the cone angle. In other terms, with such a simplified control strategy, α is allowed to attain a prescribed and finite number of values and, correspondingly, its time history is piecewise constant. As a result, the sail attitude is varied only occasionally along the trajectory. Both the number of reorientation maneuvers and their temporal spacing are chosen through an optimization process. The latter characteristic substantially differentiates the approach of Ref. [10] from that employed in a trajectory optimization with direct methods [11].

The shape of the curve $\alpha = \alpha(t)$, shown in Fig. 5, suggests the use of three different admissible values of α, that is, $(-30,\, 0,\, 30)\,\mathrm{deg}$, where $\alpha = 0$ corresponds to the maximum value of the local propulsive acceleration. For a given aphelion distance r_a, the minimum acceleration necessary to insert the spacecraft into an ERO was calculated, and its value was compared to that required by a continuous steering law, see Fig. 2. The increase Δa_c of characteristic acceleration due to the control discretization is illustrated in Fig. 6. In particular, the figure shows that the required performance increase, associated to the piecewise constant steering law, is moderate, and always less than $0.25\,\mathrm{mm/s^2}$ for $r_a > 2\,\mathrm{AU}$ both for the ideal and the optical force model. Moreover, the increase of a_c is counterbalanced by the small number (limited to a maximum of two) of required reorientation maneuvers. In particular, Fig. 7 shows the time history of the control angle for a piecewise constant steering law with two reorientation maneuvers, for an optimal transfer toward an ERO of aphelion distance $r_a = 5.2\,\mathrm{AU}$. Accordingly, the transfer to a linear trajectory is an interesting mission application of the piecewise-constant steering law concept.

5 Extended mission analysis

The previous two-dimensional analysis is now completed by including a possible mission extension, constituted by an Earth return of the solar sail. This concept would be useful, for example, for an in depth analysis of the degradation effect of the space environment on the sail film [12,13]. To this end, the whole mission is now divided into three phases, as schematically shown in Fig. 8.

The first is the transfer phase, whose aim is to transfer the spacecraft from an initial (Earth) parking orbit to the target rectilinear orbit, and corresponds to the time interval $[t_0, t_1]$. When the spacecraft reaches the ERO's aphelion (time instant t_1), the system releases a scientific probe that begins a rectilinear motion toward the Sun, until a close approach with the star at a distance r_2 causes the probe's destruction (time instant t_2). This second phase, referred as scientific phase [1], corresponds to the time interval $[t_1, t_2]$. The last phase coincides with the Earth return of the solar sail and corresponds to the time interval between t_1 and t_3, when the sail completes its Earth rendezvous. Note that the scientific phase is contemporaneous to the return phase, and its length depends both on the ERO's characteristics and the value of r_2.

In principle, the return phase would require a flight time smaller than t_1, because the spacecraft mass is now reduced with respect to the transfer phase as a result of the probe's release. The increase of solar sail characteristic acceleration in the return phase can be calculated using a simplified mass breakdown model [14], in which the in-flight initial mass m_0 is the sum of the solar sail mass m_s and the probe mass m_p, that is

$$m_0 = m_s + m_p \tag{1}$$

The solar sail characteristic acceleration for an ideal force model [4] can be written as a function of the solar radiation pressure $P_\oplus \simeq 4.5631\,\mathrm{N/km^2}$ at $r = r_\oplus$, the sail reflective area A, and

the in-flight initial mass as

$$a_c = \frac{2\,P_\oplus\,A}{m_0} \tag{2}$$

When the probe mass fraction $\eta_p \triangleq m_p/m_0$ is introduced, from Eqs. (1)-(2) the new solar sail characteristic acceleration $\widetilde{a}_c$ is obtained:

$$\widetilde{a}_c = \frac{2\,P_\oplus\,A}{m_s} \equiv \frac{a_c}{1-\eta_p} \qquad \text{for} \qquad t > t_1 \tag{3}$$

Equation (3) states that, as expected, the solar sail characteristic acceleration increases after the probe's release, and that the ratio $\widetilde{a}_c/a_c$ grows with the probe mass fraction. However for a given a_c, the maximum of $\widetilde{a}_c$ (that is, the maximum of η_p) is constrained by the minimum allowable value of the sail assembly loading m_s/A [4]. The effect of this constraint on the performance of a mission with a return trajectory to Earth, is now addressed.

When the final time t_3 and the probe mass fraction η_p are all given, it is possible to calculate the minimum required value of a_c by solving an optimization problem with interior-point constraints [15]. In particular, unlike the previous optimization problem, in this case the interior constraints concern the rectilinear orbit reaching at t_1, and the corresponding value of aphelion distance r_a. Both t_1 and r_a are now free parameters that constitute two outputs of the optimization process. Note that a given value of t_3 corresponds to a constraint on the final spacecraft angular position θ on the ecliptic plane. Indeed, assuming that at t_0 (the end of the escape phase from the terrestrial gravitational field) the spacecraft and Earth position coincide, with $\theta(t_0) \triangleq 0$, a rendezvous between the Earth and the sail at t_3 implies that the angular position of both objects is the same. If n and $n_\oplus$ represent, respectively, the number of complete revolutions of sail and Earth around the Sun in the time interval t_3, the constraint is

$$\theta(t_3) = t_3 \sqrt{\frac{\mu_\odot}{r_\oplus^3}} - 2\,(n_\oplus - n)\,\pi \tag{4}$$

where $\mu_\odot$ is the Sun's gravitational parameter. The optimal value of a_c is now a function of the pair $(t_3,\,\eta_p)$, and the simulation results for $\eta_p < 1/3$ and $t_3 < 15.5$ years have been summarized

in Figs. 9-10. To reduce the computational effort, an ideal force model has been considered in all of the simulations.

A ten-years mission, with a scientific phase time of $(t_2 - t_1) \simeq 3\,\text{years}$ and a transfer time $t_1 \simeq 4.5\,\text{years}$, can be fulfilled with a probe mass fraction of about 15% and a characteristic acceleration $a_c \simeq 3.82\,\text{mm/s}^2$ (see Fig. 9). In this case the ERO's aphelion radius is about $r_a \simeq 6.5\,\text{AU}$. For comparative purposes, a mission without an Earth return (t_1 being equal to the previous case) can be planned using a characteristic acceleration of $3.1\,\text{mm/s}^2$, see Fig. 2. This confirms that an additional mission phase (and an additional constraint at t_3) implies an overall worsening of the sail performance.

Slightly smaller values of the characteristic acceleration can be obtained, the total probe mass fraction being the same, if an increase of the total mission time t_3 can be tolerated. The decreasing trend of a_c as a function of η_p, see Fig. 9, is substantially connected to the corresponding increase of $\widetilde{a}_c$ in Eq. (3). In fact, an increase of the characteristic acceleration after the probe's release corresponds to a velocity increase of the return phase. Having fixed the total mission time t_3, an increase of $\widetilde{a}_c$ corresponds to an increase of t_1, that is, the transfer time. The latter causes a decrease in the acceleration at launch, as illustrated in Fig. 2.

The apparent performance increase after the probe's release must be evaluated with care. In fact, according to Eq. (3), an increase of η_p implies, for a given value of m_0, a corresponding decrease of the sail assembly loading m_s/A, whose minimum value is constrained by technological limits [4]. This aspect is clearly illustrated in Fig. 11, which shows the ratio m_s/A as a function of the total mission time t_3 and the payload mass fraction η_p.

Figure 11 shows, for example, that for $\eta_p = 0.15$ and $t_3 \simeq 10\,\text{years}$ the required value of sail assembly loading is slightly greater than $2\,\text{g/m}^2$. Such a value is typical of a high performance solar sail: as a matter of fact it is an order of magnitude smaller than the current technological capabilities [16,17]. A combined use of Figs. 9–11 allows one to obtain a tradeoff analysis

between the characteristics of the target ERO and the performance required by the propulsion system in a mission scenario with an Earth return.

6 Three-dimensional trajectories

So far only ERO trajectories belonging to the ecliptic plane have been investigated. In this section the assumption of two-dimensional motion is relaxed, and the ERO can now attain a suitable inclination i with respect to the ecliptic plane. This new mission scenario is particularly important as it permits to investigate, in a parametric way, the optimal spacecraft performance required to reach a purely radial trajectory with a heliocentric latitude different from zero. In particular, these kind of trajectories can be employed for a three-dimensional investigation of either the interstellar dust [18,19] or the solar wind [20].

Assuming an initial ecliptic circular orbit with a radius $r_0 = r_\oplus$ and an inclination i, the transfer performance (in terms of minimum characteristic acceleration as a function of t_1) is the same for both positive and negative values of i. Therefore, the following analysis is confined to $i > 0$. Taking into account the results for the two-dimensional case, the transfer time t_1 is assumed to not exceed 10 years. Also, the extended mission phase is not taken into account for the sake of reducing the required number of simulations. The results are summarized in Fig. 12. For a given value of flight time t_1, the characteristic acceleration increases with an increase of the final orbital inclination. Recall that the aphelion distance is left free and its value can be read from Fig. 13. For example, assuming an inclination $i = 20$ deg, the minimum flight time for a solar sail with $a_c = 3\,\mathrm{mm/s^2}$ is about 6.4 years. The trajectory corresponding to the whole mission is drawn in Fig. 14. The time variations of the distance from the Sun r, the heliocentric longitude λ (with $\lambda_0 \triangleq \lambda(t_0)$), and the latitude γ, are shown in Fig. 15. Note that once the scientific probe is released, at a distance $r_a \simeq 9.3$ AU, the probe takes about 5 years to reach the final distance $r_2 = 0.1$ AU from the Sun.

7 Conclusions

Missions towards elliptic rectilinear orbits have been studied in a parametric way. Different mission typologies have been investigated and a possible Earth return trajectory of the solar sail has been discussed. The simulations results have been collected in graphs that can be used for obtaining a first estimate of the solar sail performance required to accomplish the mission, as well as for tradeoff analysis purposes. The insertion into an elliptic rectilinear orbit requires a characteristic acceleration of about $3\,\mathrm{mm/s^2}$, which corresponds to a high performance solar sail. Although such a value is beyond the current technology capabilities, the performance necessary to reach an elliptic rectilinear orbit is significantly smaller than that required by other exotic missions, such as those regarding heliostationary orbits or those involving the orbital angular momentum reversal.

Acknowledgments

This research was financed in part by a "Paolo Manes" grant. Alessandro A. Quarta gratefully acknowledges the support of the Manes family.

References

[1] A. A. Quarta, G. Mengali, Solar sail capabilities to reach elliptic rectilinear orbits, Journal of Guidance, Control, and Dynamics 34 (3) (2011) 923–926, doi: 10.2514/1.51638.

[2] G. Colombo, D. A. Lautman, G. Pettengill, An alternative option to the dual-probe out-of-ecliptic mission via Jupiter swingby, in: Proc. of the Symp. on the Study of the Sun and Interplanetary Medium in Three Dimensions, no. N76-24119 14-92, NASA GSFC, 1976, pp. 37–47, available online (cited March 1, 2011) `http://hdl.handle.net/2060/19760017033`.

[3] J. L. Wright, Space Sailing, Gordon and Breach Science Publisher, Berlin, 1992, pp. 223–226.

[4] C. R. McInnes, Solar Sailing: Technology, Dynamics and Mission Applications, Springer-Praxis Series in Space Science and Technology, Springer-Verlag, Berlin, 1999, pp. 32–55.

[5] I. Dandouras, B. Pirard, J. Y. Prado, High performance solar sails for linear trajectories and heliostationary missions, Advances in Space Research 34 (1) (2004) 198–203, doi: 10.1016/j.asr.2003.02.055.

[6] G. Mengali, A. A. Quarta, Optimal heliostationary missions of high-performance sailcraft, Acta Astronautica 60 (8–9) (2007) 676–683, doi: 10.1016/j.actaastro.2006.07.018.

[7] G. Vulpetti, Sailcraft at high speed by orbital angular momentum reversal, Acta Astronautica 40 (10) (1997) 733–758, doi: 10.1016/S0094-5765(97)00153-7.

[8] G. Vulpetti, 3d high-speed escape heliocentric trajectories by all-metallic-sail low-mass sailcraft, Acta Astronautica 39 (1–4) (1996) 161–170, doi: 10.1016/S0094-5765(96)00133-6.

[9] G. Mengali, A. A. Quarta, Optimal three-dimensional interplanetary rendezvous using nonideal solar sail, Journal of Guidance, Control, and Dynamics 28 (1) (2005) 173–177, doi: 10.2514/1.8325.

[10] G. Mengali, A. A. Quarta, Solar sail trajectories with piecewise-constant steering laws, Aerospace Science and Technology 13 (8) (2009) 431–441, doi: 10.1016/j.ast.2009.06.007.

[11] M. Otten, C. R. McInnes, Near minimum-time trajectories for solar sails, Journal of Guidance, Control, and Dynamics 24 (3) (2001) 632–634, doi: 10.2514/2.4758.

[12] B. Dachwald, M. Macdonald, C. R. McInnes, G. Mengali, A. A. Quarta, Impact of optical degradation on solar sail mission performance, Journal of Spacecraft and Rockets 44 (4) (2007) 740–749, doi: 10.2514/1.21432.

[13] B. Dachwald, G. Mengali, A. A. Quarta, M. Macdonald, Parametric model and optimal control of solar sails with optical degradation, Journal of Guidance, Control, and Dynamics 29 (5) (2006) 1170–1178, doi: 10.2514/1.20313.

[14] G. Mengali, A. A. Quarta, Solar-sail-based stopover cyclers for cargo transportation missions, Journal of Spacecraft and Rockets 44 (4) (2007) 822–830, doi: 10.2514/1.24423.

[15] A. E. Bryson, Y. C. Ho, Applied Optimal Control, Hemisphere Publishing Corporation, New York, NY, 1975, Ch. 2, pp. 71–89, 101–110.

[16] B. Dachwald, W. Seboldt, Multiple near-earth asteroid rendezvous and sample return using first generation solar sailcraft, Acta Astronautica 57 (11) (2005) 864–875, doi: 10.1016/j.actaastro.2005.04.012.

[17] B. Dachwald, W. Seboldt, L. Richter, Multiple rendezvous and sample return missions to near-earth objects using solar sailcraft, Acta Astronautica 59 (8-11) (2006) 768–776, doi: 10.1016/j.actaastro.2005.07.061.

[18] M. Baguhl, E. Grun, M. Landgraf, In situ measurements of interstellar dust with the Ulysses and Galileo spaceprobes, Space Science Reviews 78 (1-2) (1996) 165–172, doi: 10.1007/BF00170803.

[19] I. Mann, A. Krivov, H. Kimura, Dust cloud near the sun, Icarus 146 (2) (2000) 568–582, doi: 10.1006/icar.2000.6419.

[20] R. J. Macdowall, M. D. Desch, M. L. Kaiser, R. G. Stone, R. A. Hess, A. Balogh, S. J. Bame, B. E. Goldstein, The three-dimensional extent of a high speed solar wind stream, Space Science Reviews 72 (1–2) (1995) 125–128, doi: 10.1007/BF00768767.

List of Figures

1 Bi-impulsive, Hohmann-like, Earth-to-ERO heliocentric transfer. 16

2 Optimal performance for a two-dimensional Earth-to-ERO heliocentric transfer using a flat solar sail with an ideal (solid line) and optical (dashed line) force model. 17

3 Mission trajectory for $r_a = 5.2\,\mathrm{AU}$, $t_1 = 2.85\,\mathrm{years}$, and $a_c = 3.52\,\mathrm{mm/s^2}$ (marks are shown with 30 days apart). 18

4 Sun-sail distance r and velocity components u and v for an optimal trajectory with $r_a = 5.2\,\mathrm{AU}$, $t_1 = 2.8\,\mathrm{years}$, and $a_c = 3.52\,\mathrm{mm/s^2}$ (ideal force model). 19

5 Cone angle time history for $r_a = 5.2\,\mathrm{AU}$, $t_1 = 2.8\,\mathrm{years}$, and $a_c = 3.52\,\mathrm{mm/s^2}$ (ideal force model). 20

6 Characteristic acceleration increase, and number of reorientation maneuvers, associated to a piecewise-constant steering law in a two-dimensional transfer. 21

7 Time-history of piecewise-constant steering law for a transfer toward an ERO with $r_a = 5.2\,\mathrm{AU}$ using an ideal force model. Dashed line refers to continuous control law. 22

8 Extended mission concept with an Earth return phase. 23

9 Optimal performance for a mission with an Earth return with an ideal force model. 24

10 Flight times for a mission with an Earth return with an ideal force model. 25

11 Sail assembly loading for a mission with an Earth return with an ideal force model. 26

12 Three-dimensional transfer performance as a function of t_1, and i using an ideal force model. 27

13 Probe's release distance r_a as a function of t_1 and a_c using an ideal force model. 28

14 Mission trajectory for $a_c = 3\,\mathrm{mm/s^2}$, $i = 20\,\mathrm{deg}$, and $r_a = 9.3\,\mathrm{AU}$ (ideal force model). 29

15 Time variation of position parameters for $a_c = 3\,\mathrm{mm/s^2}$, $u_1 = 0$, and $r_2 = 0.1$ AU (ideal force model). 30

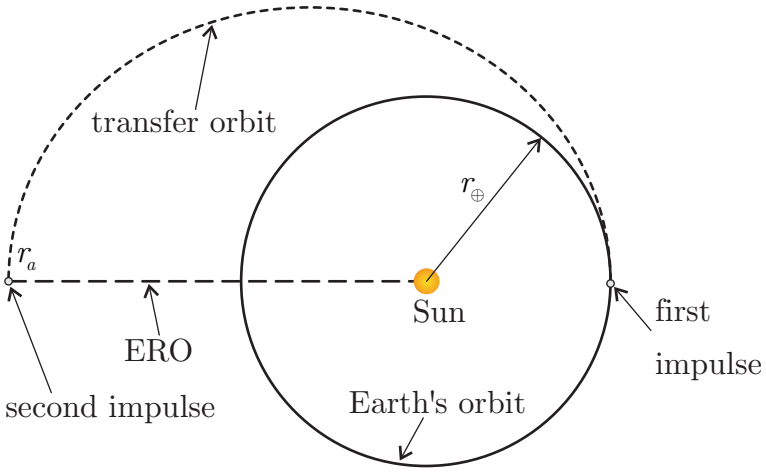

(a) Transfer scenario.

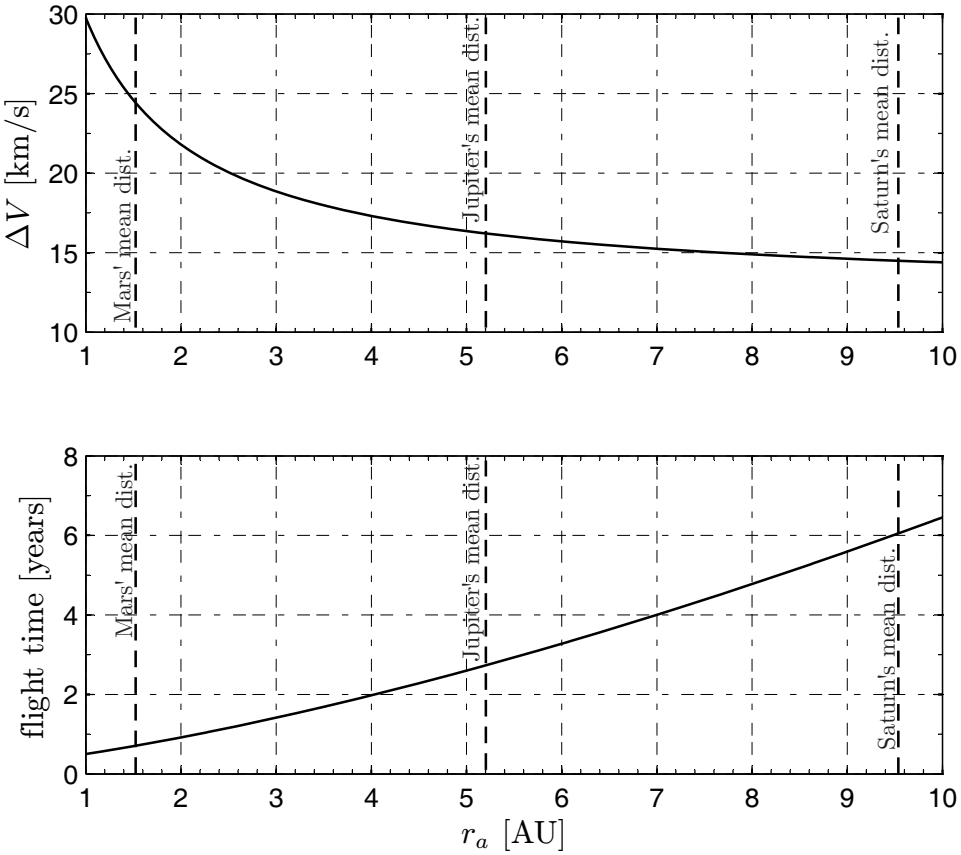

(b) Transfer performance.

Figure 1. Bi-impulsive, Hohmann-like, Earth-to-ERO heliocentric transfer.

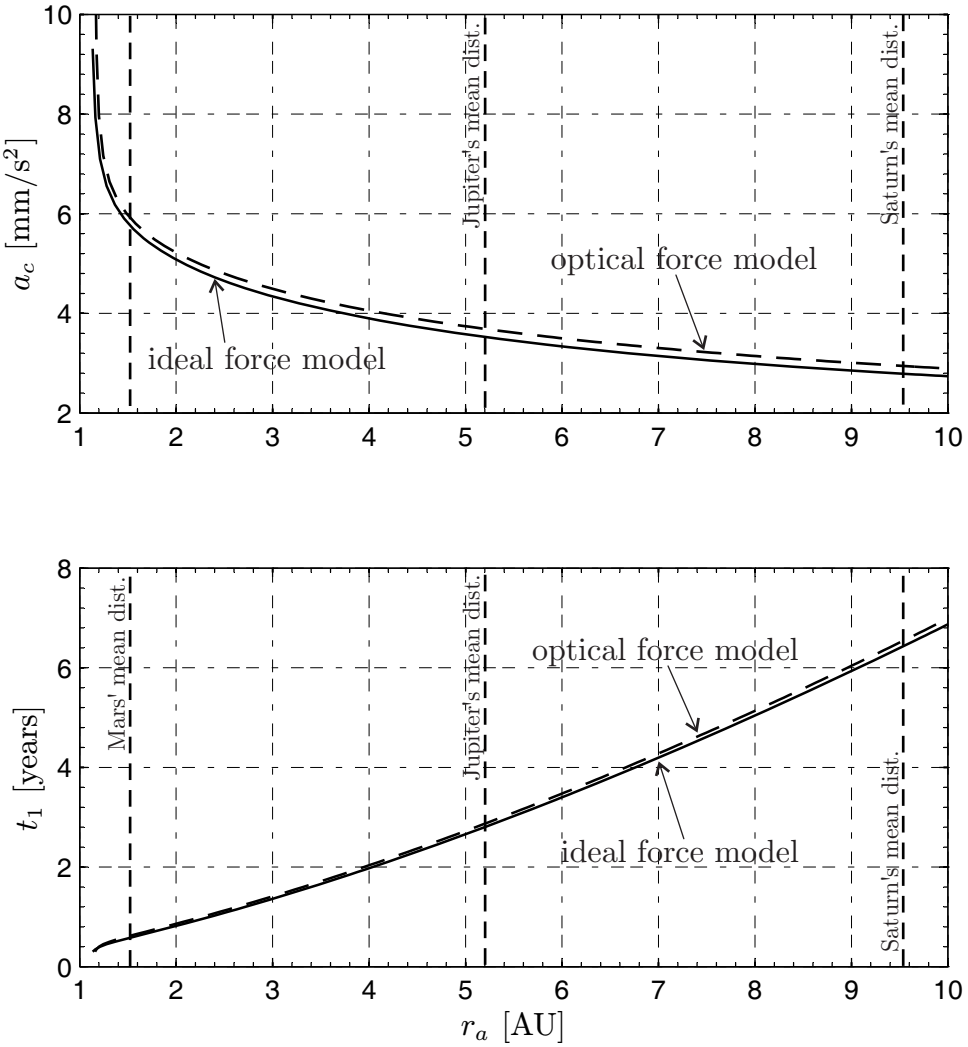

Figure 2. Optimal performance for a two-dimensional Earth-to-ERO heliocentric transfer using a flat solar sail with an ideal (solid line) and optical (dashed line) force model.

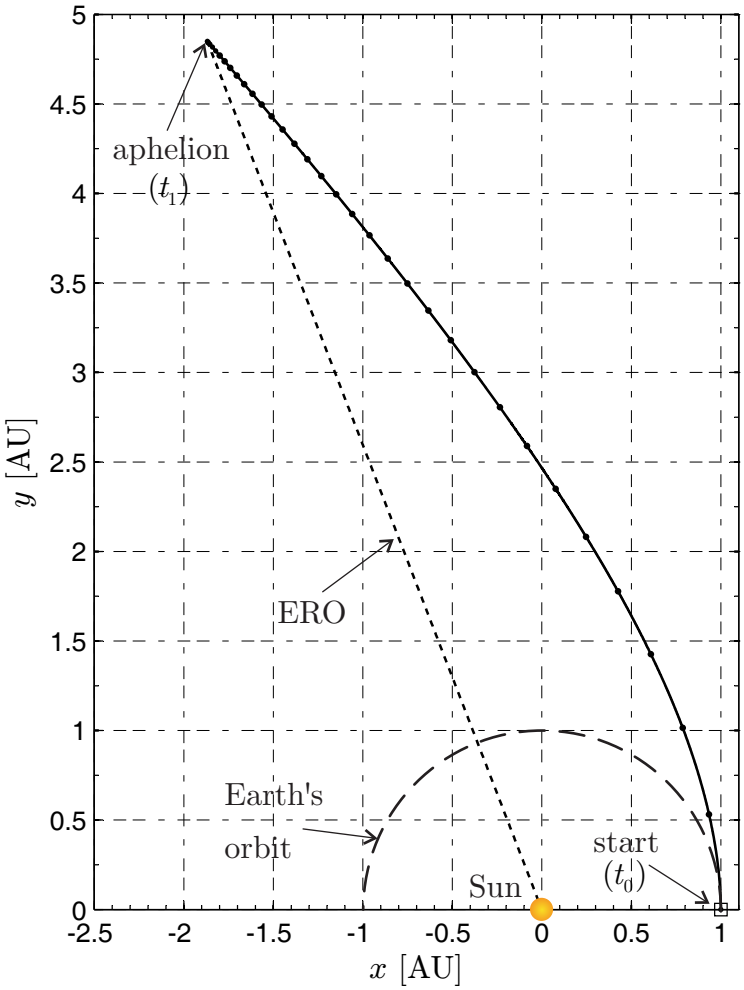

Figure 3. Mission trajectory for $r_a = 5.2\,\mathrm{AU}$, $t_1 = 2.85\,\mathrm{years}$, and $a_c = 3.52\,\mathrm{mm/s^2}$ (marks are shown with 30 days apart).

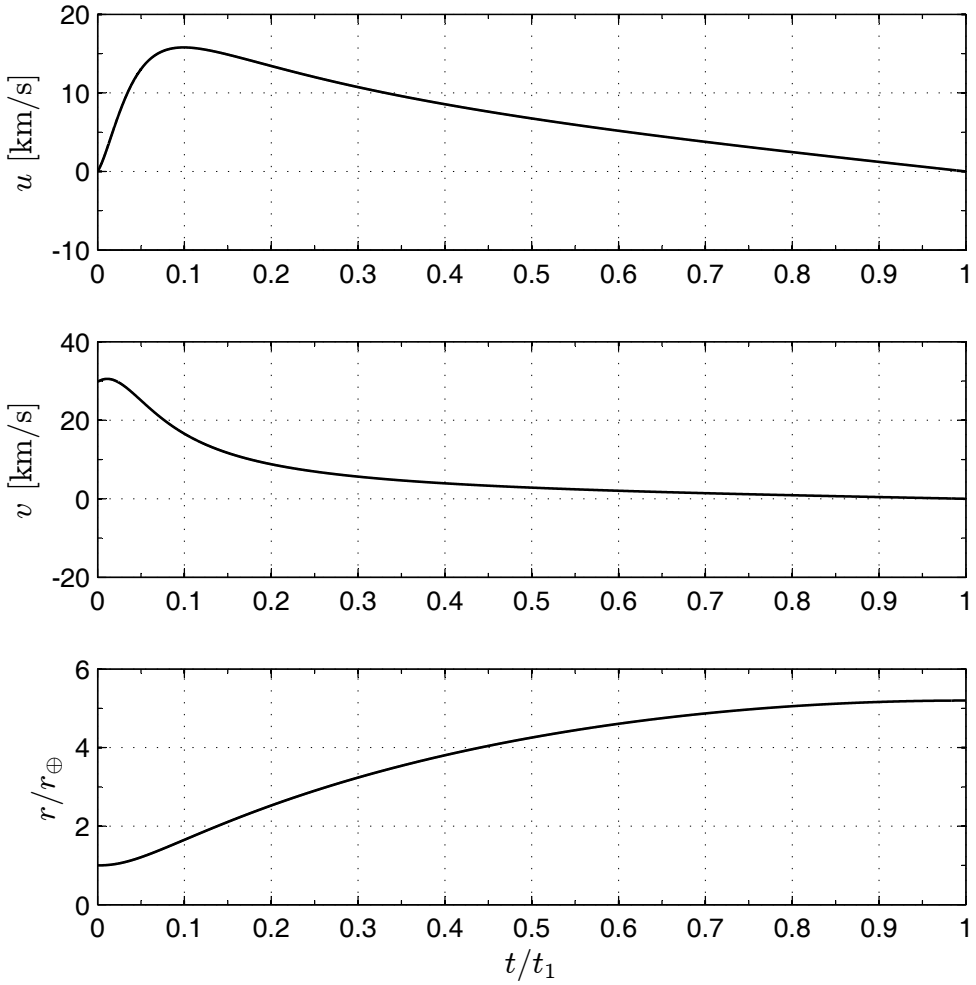

Figure 4. Sun-sail distance r and velocity components u and v for an optimal trajectory with $r_a = 5.2\,\mathrm{AU}$, $t_1 = 2.8\,\mathrm{years}$, and $a_c = 3.52\,\mathrm{mm/s^2}$ (ideal force model).

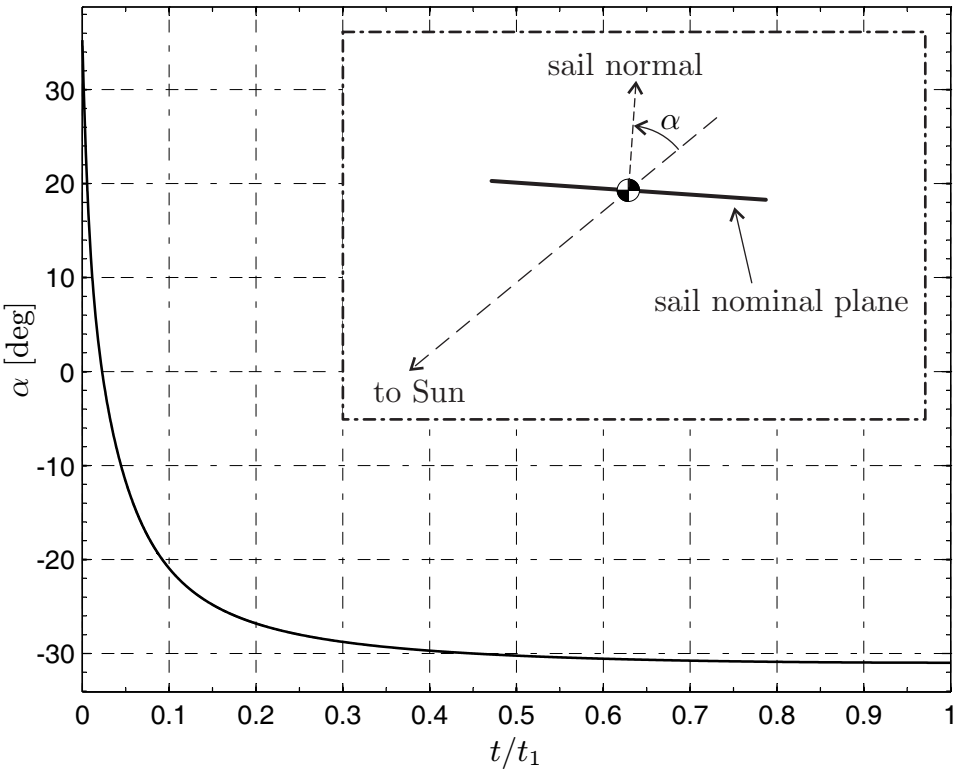

Figure 5. Cone angle time history for $r_a = 5.2\,\mathrm{AU}$, $t_1 = 2.8\,\mathrm{years}$, and $a_c = 3.52\,\mathrm{mm/s^2}$ (ideal force model).

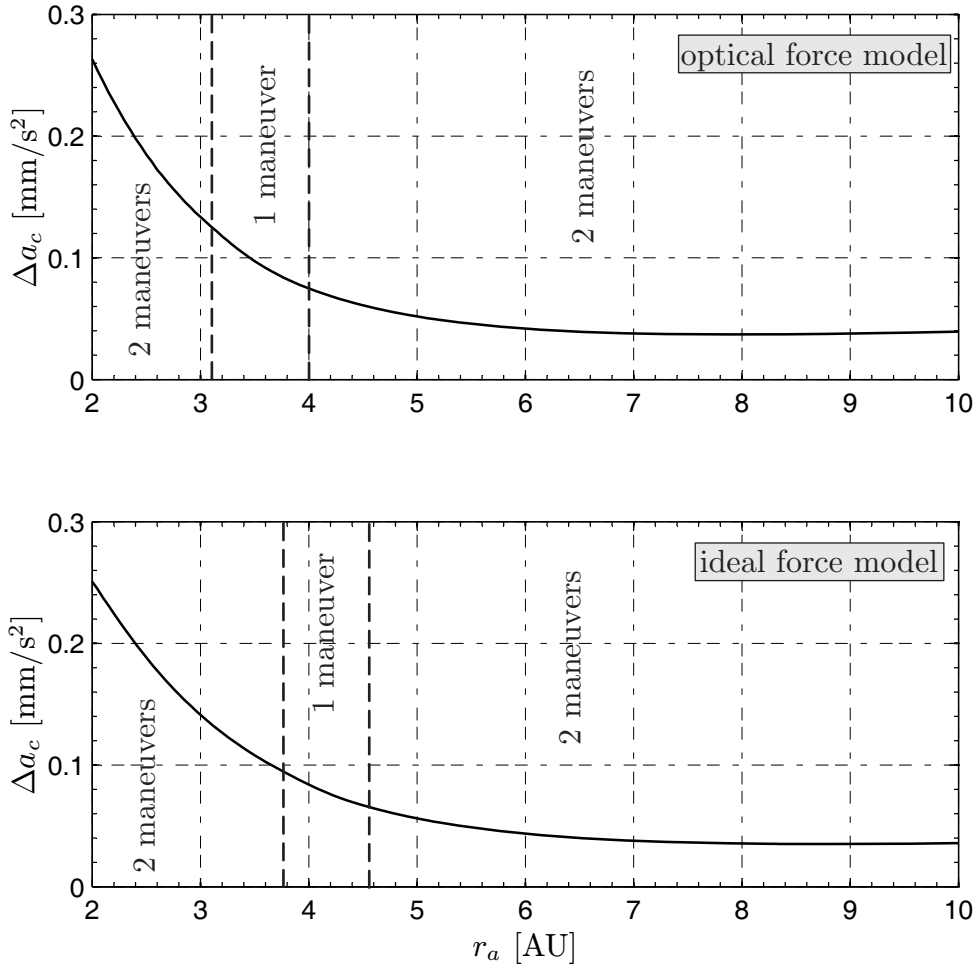

Figure 6. Characteristic acceleration increase, and number of reorientation maneuvers, associated to a piecewise-constant steering law in a two-dimensional transfer.

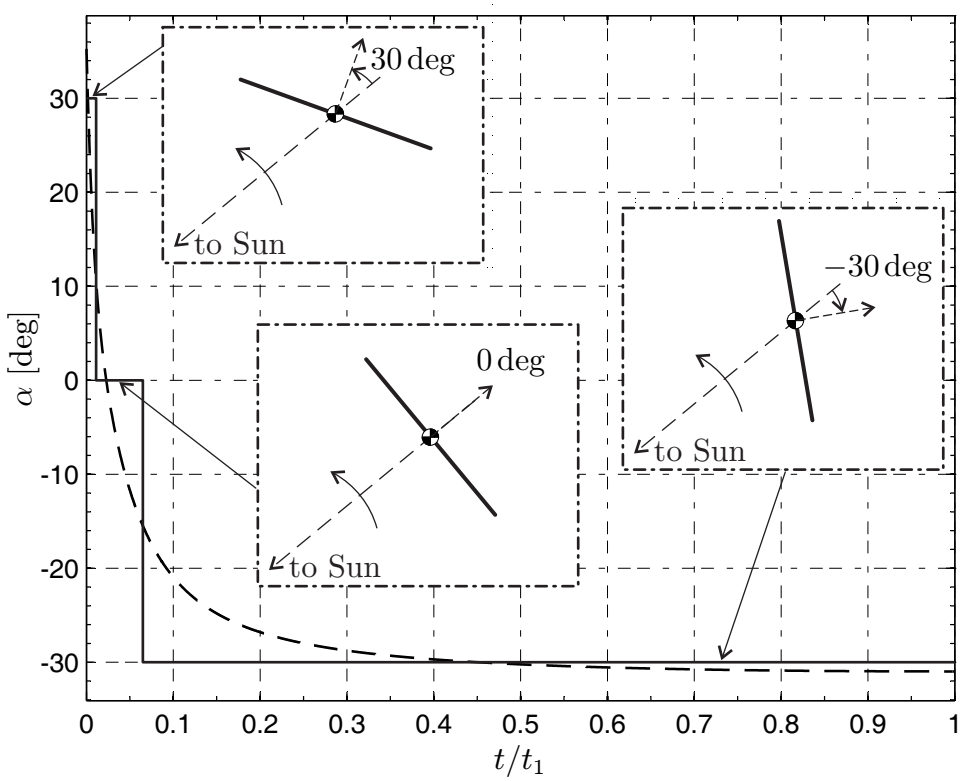

Figure 7. Time-history of piecewise-constant steering law for a transfer toward an ERO with $r_a = 5.2\,\mathrm{AU}$ using an ideal force model. Dashed line refers to continuous control law.

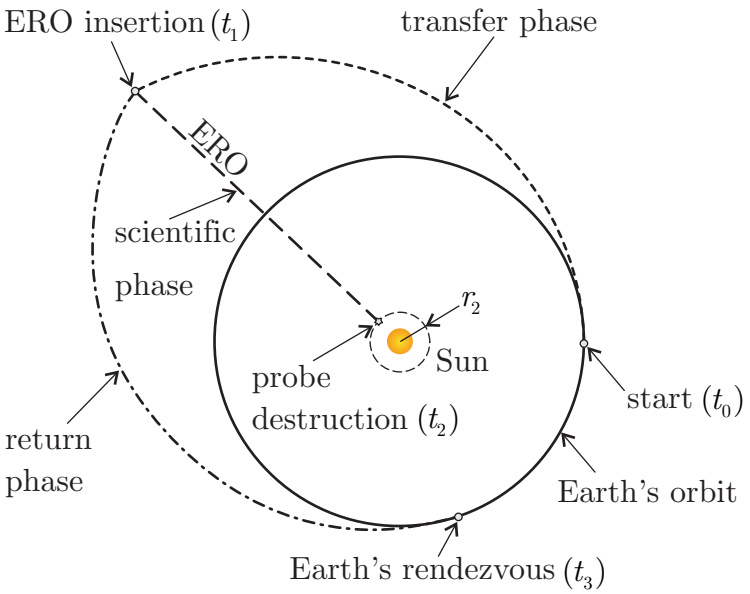

Figure 8. Extended mission concept with an Earth return phase.

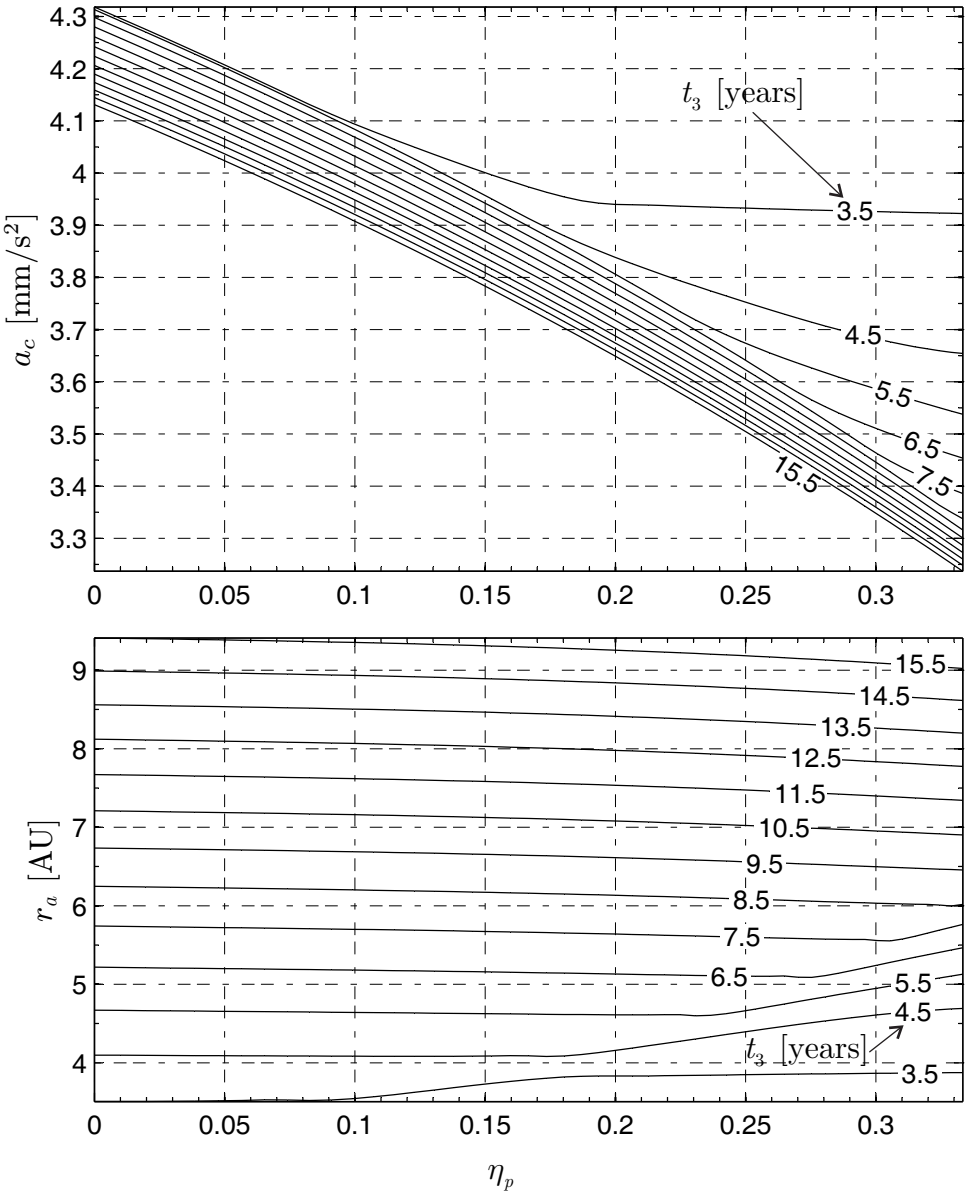

Figure 9. Optimal performance for a mission with an Earth return with an ideal force model.

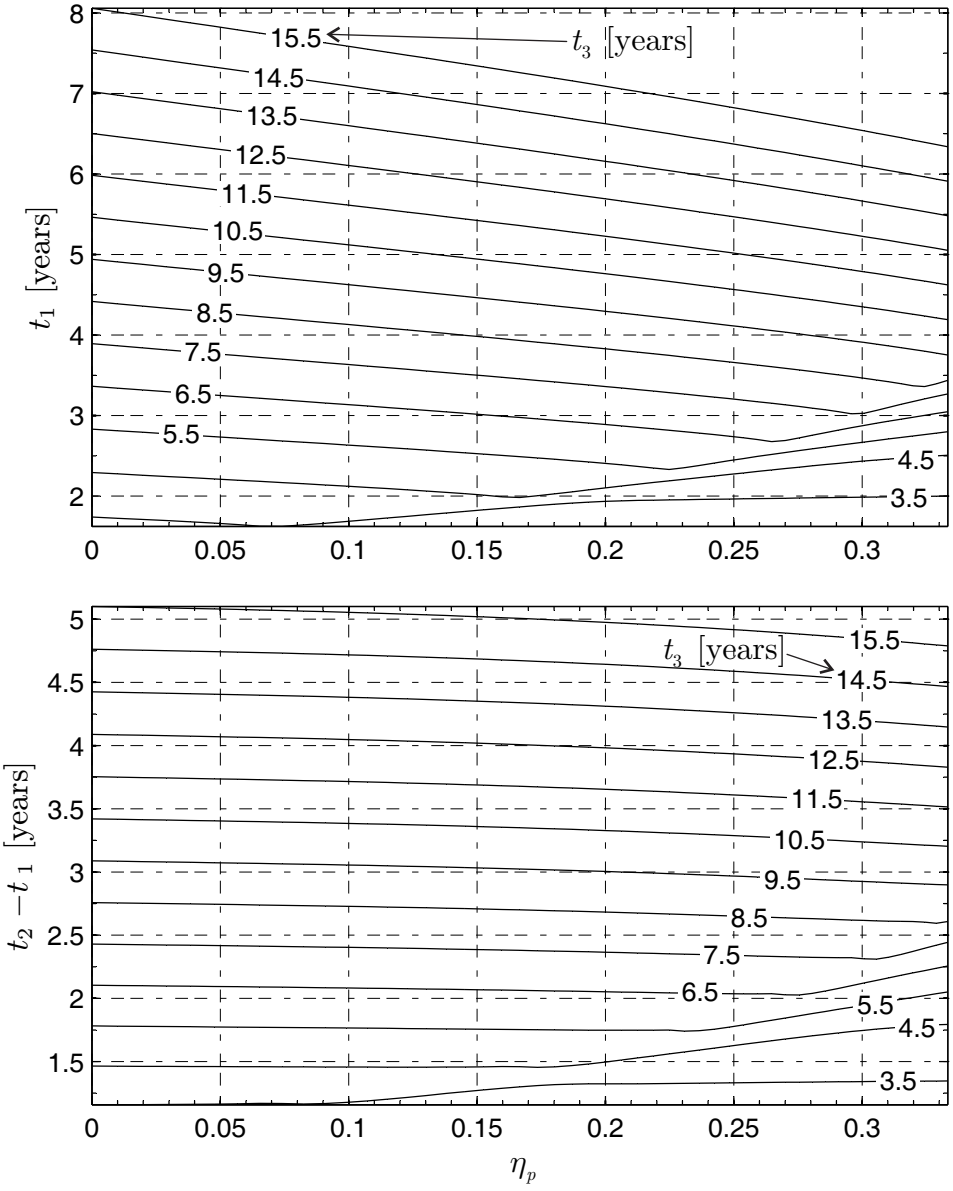

Figure 10. Flight times for a mission with an Earth return with an ideal force model.

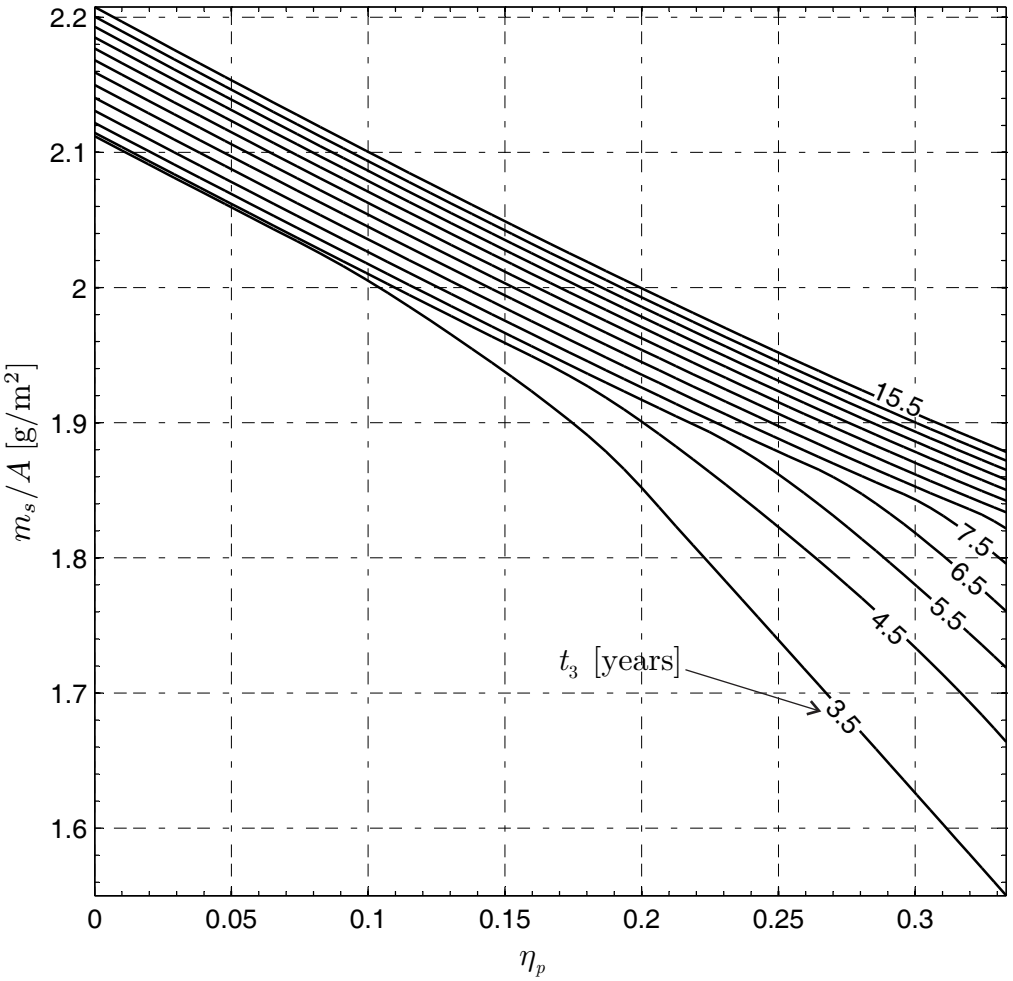

Figure 11. Sail assembly loading for a mission with an Earth return with an ideal force model.

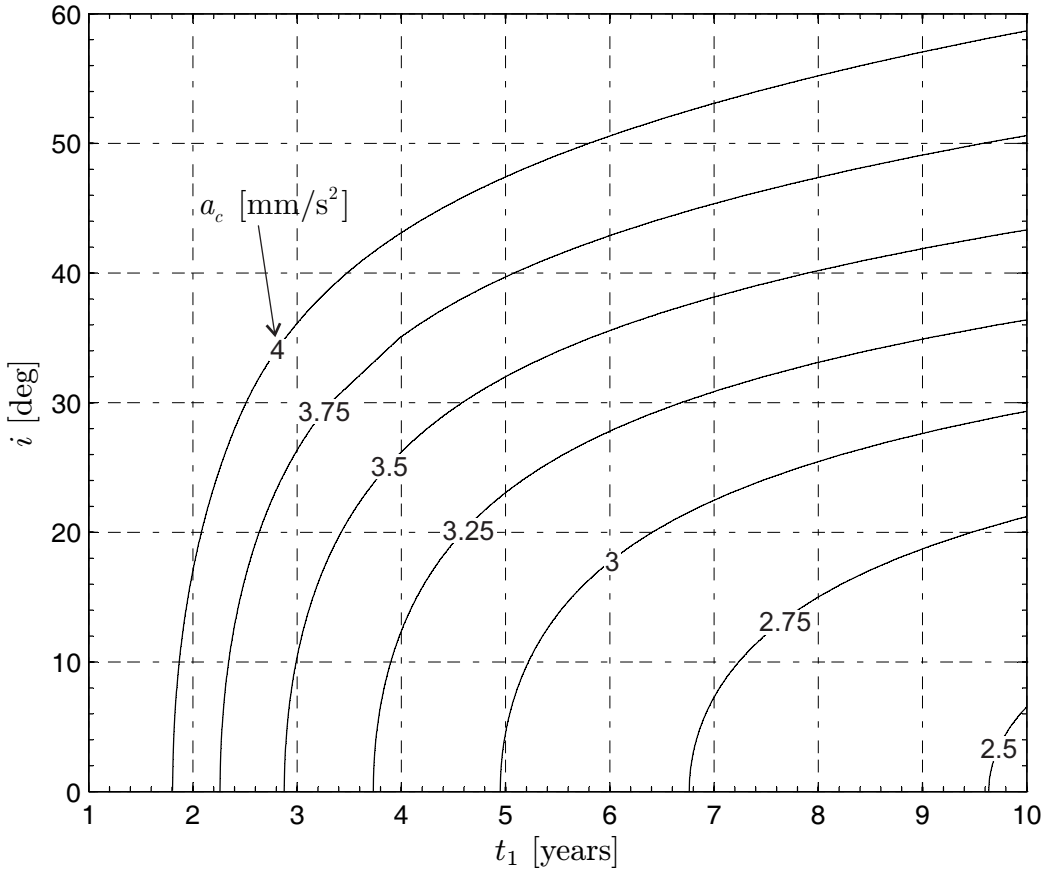

Figure 12. Three-dimensional transfer performance as a function of t_1, and i using an ideal force model.

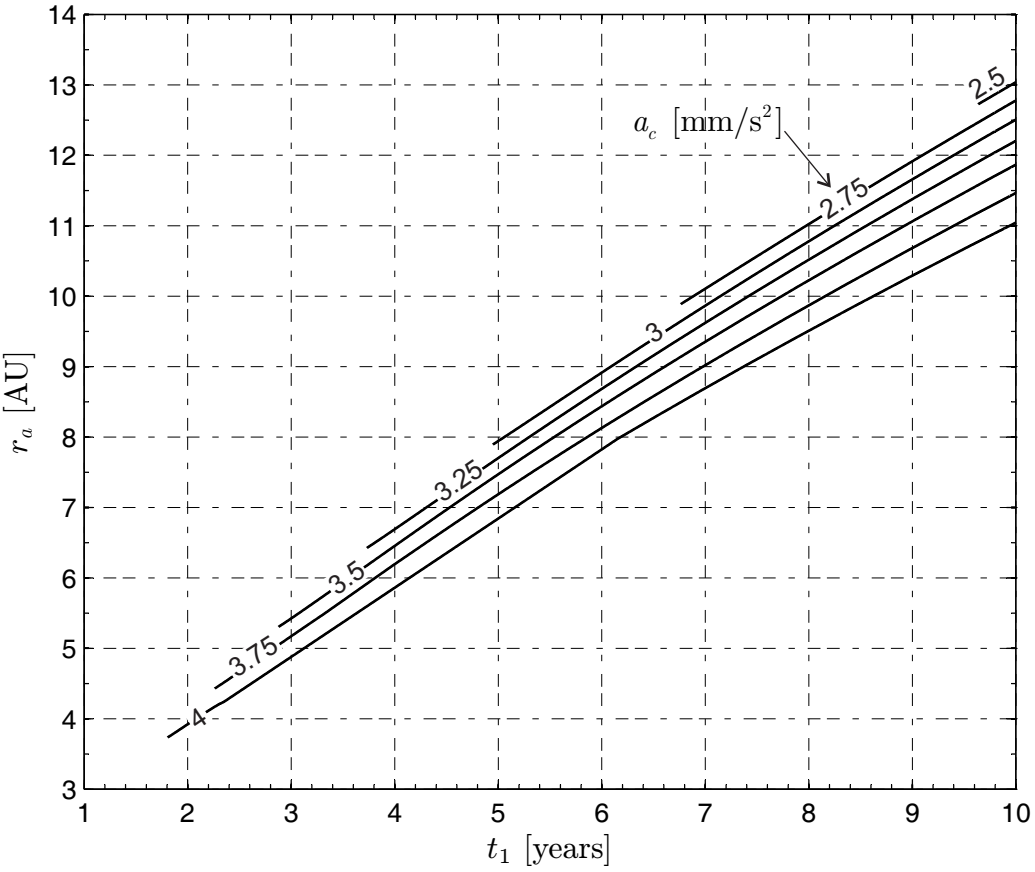

Figure 13. Probe's release distance r_a as a function of t_1 and a_c using an ideal force model.

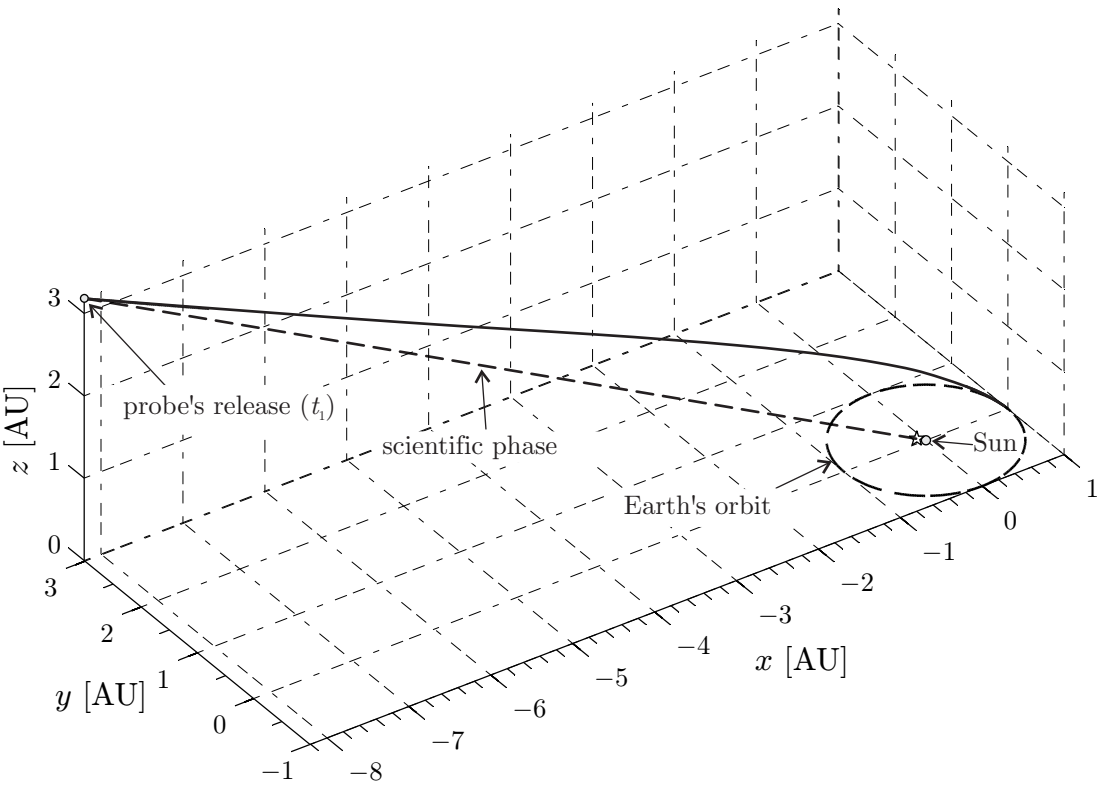

Figure 14. Mission trajectory for $a_c = 3\,\mathrm{mm/s^2}$, $i = 20\,\mathrm{deg}$, and $r_a = 9.3\,\mathrm{AU}$ (ideal force model).

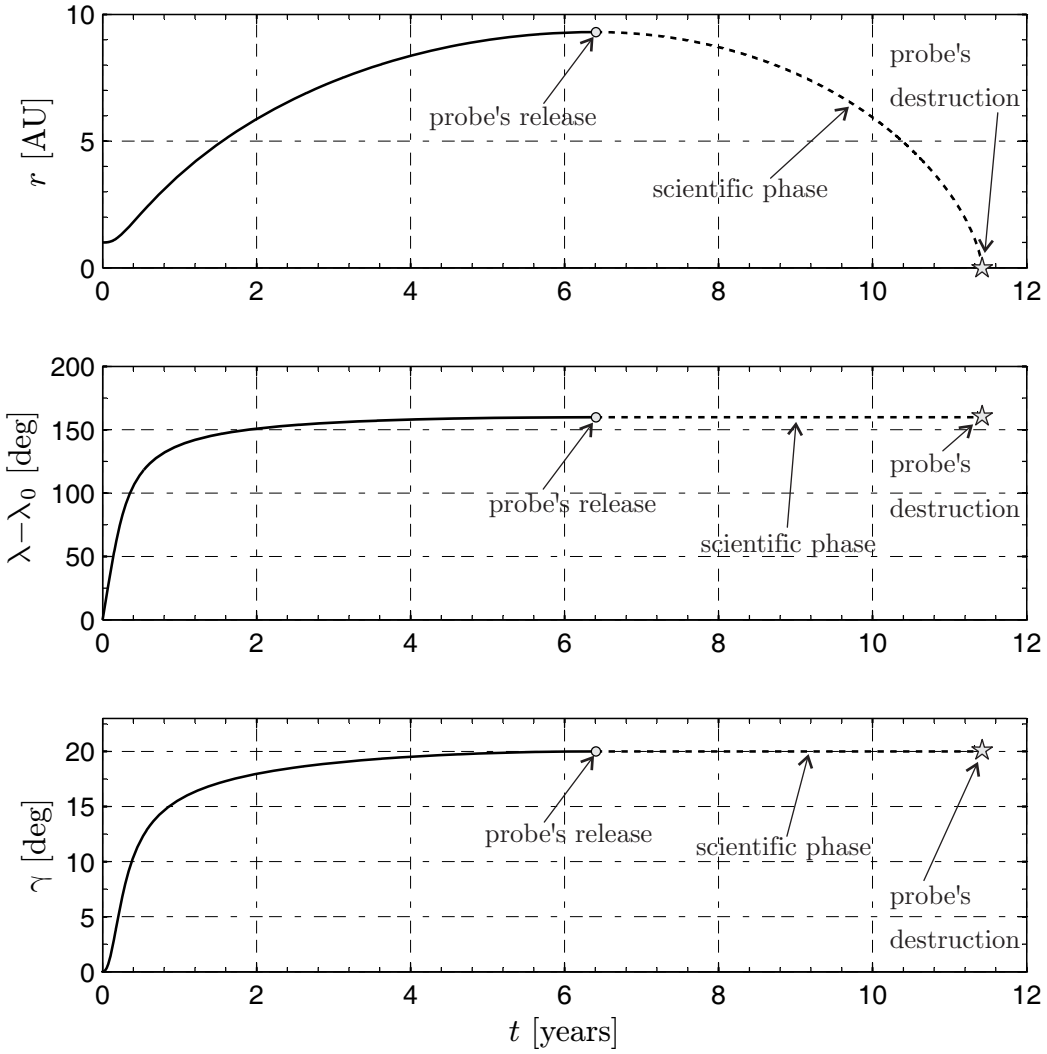

Figure 15. Time variation of position parameters for $a_c = 3\,\mathrm{mm/s^2}$, $u_1 = 0$, and $r_2 = 0.1$ AU (ideal force model).